Inorganic Chemistry

Article

pubs.acs.org/IC

Role of Tyrosine Residue in Methane Activation at the Dicopper Site of Particulate Methane Monooxygenase: A Density Functional Theory Study

Yoshihito Shiota, Gergely Juhász, and Kazunari Yoshizawa*

Institute for Materials Chemistry and Engineering and International Research Center for Molecular System, Kyushu University, Fukuoka 819-0395, Japan

Supporting Information

ABSTRACT: Methane hydroxylation at the dinuclear copper site of particulate methane monooxygenase (pMMO) is studied by using density functional theory calculations. The electronic, structural, and reactivity properties of a possible dinuclear copper species (μ-oxo)(μ-hydroxo)$Cu^{II}Cu^{III}$ are discussed with respect to the C−H bond activation of methane. We propose that the tyrosine residue in the second coordination sphere of the dicopper site donates an H atom to the μ-η^2:η^2-peroxo$Cu^{II}Cu^{II}$ species and the resultant (μ-oxo)(μ-hydroxo)$Cu^{II}Cu^{III}$ species can hydroxylate methane. This species for methane hydroxylation is more favorable in reactivity than the bis(μ-oxo)$Cu^{III}Cu^{III}$ species. The H-atom transfer or proton-coupled electron transfer from the tyrosine residue can reasonably induce the O−O bond dissociation of the μ-η^2:η^2-peroxo$Cu^{II}Cu^{II}$ species to form the reactive (μ-oxo)(μ-hydroxo)$Cu^{II}Cu^{III}$ species, which is expected to be an active species for the conversion of methane to methanol at the dicopper site of pMMO. The rate-determining step for the methane hydroxylation is the C−H cleavage, which is in good agreement with experimental KIE values reported so far.

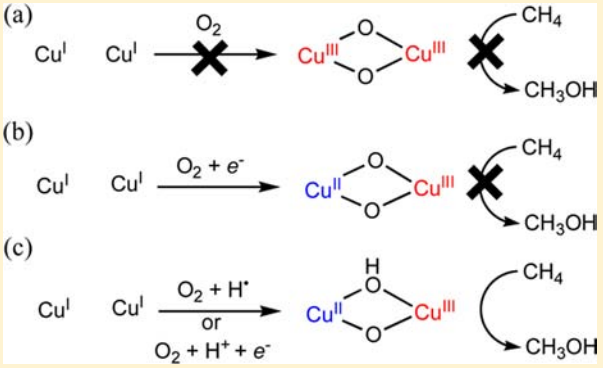

INTRODUCTION

The biological conversion of methane-to-methanol by methane monooxygenase (MMO) is an important enzymatic function[1,2] under mild conditions because the activation of the strong C−H bond in methane requires high-pressure (40 atm) and high-temperature (850 °C) conditions in the presence of nickel catalyst in the industrial two-step methane-methanol production via the formation of CO and H_2.[3] The methanotrophic bacteria use MMO that has two different forms depending on the level of copper ion in the soil. Under low levels of copper ion, the cells express only soluble MMO (sMMO) in the cytoplasm. Above a copper ion concentration >4 μM, the cells switch to use a membrane protein, particulate MMO (pMMO). The two enzymatic systems show significant differences in their structures and in their metal active sites. In sMMO, methane hydroxylation is performed at a diiron active site,[4] and a large number of studies have been performed on the function of the active site of sMMO using various spectroscopic measurements. From quantum chemical calculations, nonradical,[5] radical,[6,7] and nonsynchronous concerted[8] mechanisms have been proposed for methane hydroxylation by sMMO. In contrast, little is known about the structure of the protein environment and the location of copper active sites of pMMO, a multi copper protein.[9−11] In 2005 Lieberman and Rosenzweig[11a] reported an X-ray crystal structural analysis of pMMO at 2.8 Å resolution. Their excellent work revealed that pMMO consists of three subunits of pmoA, pmoB, and pmoC. This analysis has identified three different metal centers in pMMO. The pmoB subunit contains a mononuclear copper site and a dinuclear copper site. Between pmoA and pmoC, a monozinc site is located 19 Å apart from the dicopper site and 32 Å apart from the monocopper site. Since zinc is contained in the crystallization buffer used and not detected in X-ray absorption spectroscopy (XAS) measurements,[12] this site is considered to be occupied by a different metal ion such as iron or copper in vivo. The involvement of nonheme iron for methane hydroxylation by pMMO has been discussed so far;[13] for example, on the basis of Mössbauer spectroscopy, Münck and co-workers[13c] reported that pMMO should contain a dinuclear iron species. Chan and co-workers[14] proposed an active site that is composed of a trinuclear $Cu^{II}Cu^{II}Cu^{II}$ cluster based on results of X-ray adsorption edge and electron spin resonance spectroscopic experiments. They suggested that the active site of the X-ray crystal structure might be incomplete, for example, missing a copper ion, and the active form of the enzyme can be significantly different from the X-ray structure that does not display any enzymatic activity. Recently Chan and co-workers reported that two trinuclear synthetic complexes can actually oxidize methane.[14e] The identity of the metals in the active site

Received: February 17, 2013
Published: June 28, 2013

   dx.doi.org/10.1021/ic400417d | Inorg. Chem. 2013, 52, 7907−7917

Scheme 1

has been discussed as being about different metals like Cu[10,14] and Fe.[13] Rosenzweig and co-workers recently reported that the activity of pMMO is dependent on copper, not on iron, and that the copper active site is located in the soluble domains of the pmoB subunit at the site of the crystallographic dicopper center.[15]

By means of quantum chemical calculations,[5e,16,17] mono-, di-, and tri-copper models have been analyzed for the active site of pMMO. Chen and Chan[17] predicted that a trinuclear $Cu^{II}Cu^{II}Cu^{III}$ complex offers the most facile pathway for methane hydroxylation with a low activation energy. We have previously investigated the reaction pathway and its energetics for the direct methane-methanol conversion by a series of first-row transition-metal oxide species (from Sc to Cu) using the density functional theory (DFT) approach.[18] The FeO^+ species that is formed from the reaction between Fe^+ and N_2O is of great interest in considering the catalytic mechanism because it is the simplest oxidation catalyst for the conversion of methane to methanol in the gas phase. DFT calculations suggest that late transition-metal oxides especially FeO^+, NiO^+, and CuO^+, in which the metal centers are formally +3 in charge, are highly reactive to methane, which is fully consistent with the experimental observations.[19] These reactions involve one or two spin-crossover regions between the high-spin state and the low-spin state in the reaction energy profiles. On the basis of the X-ray crystal structure (1YEW),[11a] we constructed reaction models for the monocopper and dicopper sites.[16a] Our calculations suggested that the formation of a dicopper active species is favored from an energetic point of view.

Rosenzweig and co-workers reported that the dicopper site of pMMO should play an essential role in methane hydroxylation.[11,15] Their activity data indicate the pMMO copper active site to be located within pmoB and rule out the possibility of the active site being a diiron center located at the crystallographic zinc site or a trinuclear copper center possibly located at the intramembrane hydrophilic patch. Although the real active site of pMMO is quite controversial, the dicopper site is a most likely candidate. However, there remains an open question about what kind of $[Cu_2O_x]^{+y}$ species can activate methane at the dicopper site. Typical dicopper-oxo species referred to here are shown in Scheme 1. Although the real active species for methane hydroxylation has not yet been experimentally identified, we previously proposed that a bis(μ-oxo)$Cu^{II}Cu^{III}$ species is a possible candidate for the enzymatic methane oxidation.[5e,16] Karlin and co-workers[20] also pointed out that a mixed-valent $Cu^{II}Cu^{III}$ bis-oxo (or oxo-hydroxo) complex would be an important synthetic target for model study in copper−oxygen chemistry. In a recent spectroscopic/computational study on methane oxidation catalyzed by Cu-ZSM-5 zeolite, Solomon, Schoonheydt, and co-workers demonstrated that a (μ-oxo)$Cu^{II}Cu^{II}$ species should be an oxygenating agent.[21] Inspired by methane oxidation by Cu-ZSM-5, they proposed that the (μ-oxo)$Cu^{II}Cu^{II}$ species is also a key species for the enzymatic methane oxidation by pMMO. Yumura et al. reported the electronic structures of dioxygen at a possible dicopper site of Cu-ZSM-5,[24] suggesting that the spatial constraint from the ZSM-5 framework has a strong impact on the energy profile of dioxygen activation by Cu-ZSM-5. A number of structural and spectroscopic data about model complexes[23−25] suggest that dicopper species can be responsible for the activation of dioxygen and the oxidation of substrate. To address this question, we would like to revisit the reactivity of the dicopper active species to methane. In the present study we consider the reactivity of a dicopper species of (μ-oxo)(μ-hydroxo)$Cu^{II}Cu^{III}$, which can be derived from H-atom migration or proton-coupled electron transfer associated with a tyrosine residue in the second coordination sphere of the dicopper site of pMMO.

COMPUTATIONAL METHOD

The B3LYP method[26] has been widely used for the simulation of various catalytic and enzymatic reactions; however, it tends to overestimate the spin-state splitting.[27] This might be a serious shortcoming in the present work since the relative energy of intermediates with different spin states is a crucial question for discussing transition-metal catalyzed reactions. To avoid this problem, we used a newly parametrized version of B3LYP developed by Reiher and co-workers:[27] the B3LYP* functional with 15% Hartree−Fock exchange instead of 20% in the B3LYP functional. The B3LYP* hybrid functional was specifically developed for the calculation of accurate spin-state splitting while keeping the accuracy of the B3LYP method for other calculated parameters. We used the (16s10p6d) primitive set of Wachters−Hay supplemented with one polarization f-function (α = 1.44 for Cu)[28] for the Cu atoms and the D95** basis set[29] for the H, C, and O atoms. The program we used is Gaussian 09.[30] We used the His33, Glu35, His137, His139, and Tyr374 residues in the dicopper model and performed restrained optimizations while constraining the Cα atoms of the Glu35, His137, His139, and Tyr374 residues to their positions in the crystal structure. This constraint method is useful to reproduce the rigidity of the active site that involves some residues at the second coordination sphere. After geometry optimizations, vibrational analyses were performed for the estimation of Gibbs free energies including zero-point vibrational energies and thermal corrections at 298.15 K.

RESULTS AND DISCUSSION

Computational Model of the Dicopper Active Site. The X-ray structure of the dicopper site in the pmoB subunit is shown in Figure 1a.[11] In the previous studies we proposed a possible Cu^ICu^{II} peroxo species,[16] shown in Figure 1b, as a model of this active site. The Cu^ICu^{II} peroxo species is assumed to be formed from the original reduced Cu^ICu^I state after the addition of an oxygen molecule and the transfer of one electron. We assumed that Glu35 should coordinate to one of the copper ions, as shown in Figure 1b. Acetate is used as a model of the Glu35 residue, and imidazole molecules as a model of the three His residues. In the present study we consider a peroxo species with the $Cu^{II}Cu^{II}$ oxidation state

dx.doi.org/10.1021/ic400417d | Inorg. Chem. 2013, 52, 7907−7917

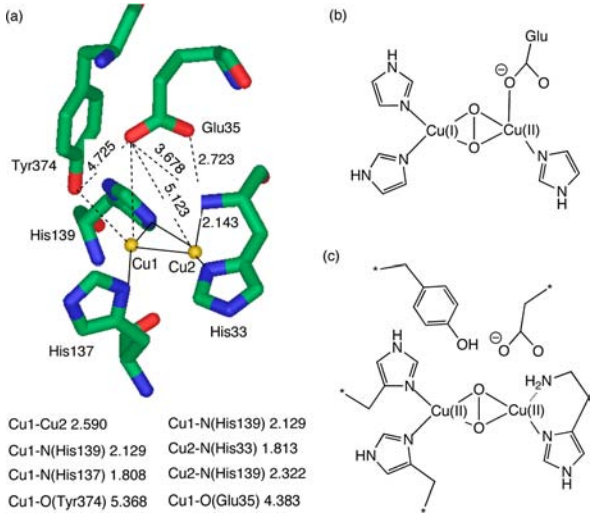

Figure 1. (a) X-ray structure of the dicopper site in the pmoB subunit of pMMO[11a] and computational models of the active site: (b) a $Cu^{I}Cu^{II}$ peroxo species[16a] and (c) a $Cu^{II}Cu^{II}$ peroxo species (this work). Distances are in angstrom (Å). The C-α atoms indicated by asterisk in the Glu35, His137, His139, and Tyr374 residues are constrained to their positions in the crystal structure. The N-terminus of His33 is not constrained.

containing one Tyr residue, one Glu residue, and three His residues, as shown in Figure 1c. Here we focus on the role of the Tyr374 residue outside the first coordination sphere of the dicopper site. Although the Tyr374 residue in 1YEW[11a] is not structurally conserved in pMMOs from *Methylosinus trichosporium* OB3b (3CHX)[11c] and *Methylocystis* sp. strain M (3RFR),[11d] the two pMMOs contain tyrosine residues (Tyr352 and Tyr341) near the dicopper active site, respectively. The tyrosine residues of 3CHX and 3RFR are likely to work in the catalysis in a similarly way to Tyr374 of 1YEW. Our discussion about the involvement of Tyr374 in the reactivity would be also applicable in other pMMOs.

We previously reported that the H-atom transfer from tyrosine to the side-on peroxo species of tyrosinase, which leads to the formation of a (μ-oxo)(μ-hydroxo)$Cu^{II}Cu^{III}$ species, plays an important role in the oxidation of tyrosine to dopaquinone.[31] The H-atom transfer effectively initiates the cleavage of the peroxo O−O bond, which is an essential process in oxygenation enzymes using O_2 as an oxidant, and significantly increases the reactivity of the resultant (μ-oxo)(μ-hydroxo)$Cu^{II}Cu^{III}$ species. On the basis of the proposed mechanism of tyrosinase, we considered a similar H-atom transfer to initiate the O−O bond cleavage, which leads to the formation of the active (μ-oxo)(μ-hydroxo)$Cu^{II}Cu^{III}$ species in pMMO. In the present work we set up a cluster model of the enzyme active center of 1YEW to look at the reactivity of the possible dicopper species. Using a cluster model by constraining C-α atoms to crystallographic coordinates is one way of looking at the reactivity of enzyme active sites and has been widely used. The C-α atoms of the Glu35, His137, His139, and Tyr374 residues are fixed to their positions in the crystal structure. Although the present DFT calculations do not explicitly include protein environmental effects, this approach can reasonably describe the reaction between active site and substrate. The N-terminus of the His33 residue is not constrained. The terminal histidine acts as a bidentate ligand to a copper atom in the dicopper site of pMMO; the Cu−N bond remains almost unchanged during the oxidation reaction in the DFT calculations. Mononuclear copper enzymes[32] also contain this kind of terminal histidine as a ligand at the copper active site.

Electronic Structures of Possible Intermediates. We show in Figure 2 optimized structures and free enthalpies of the $Cu^{I}Cu^{I}$ (**RED**), μ-η^2:η^2-peroxo$Cu^{II}Cu^{II}$ (**PO**), μ-η^1:η^2-hydroperoxo$Cu^{I}Cu^{II}$ (**HPO**), bis(μ-oxo)$Cu^{III}Cu^{III}$ (**BMO**), and (μ-oxo)(μ-hydroxo)$Cu^{II}Cu^{III}$ (**OHO**) intermediates in a proposed reaction mechanism. The reduced form of the enzyme model is **RED**, which is a diamagnetic $Cu^{I}Cu^{I}$ species corresponding to a pair of d^{10} (closed-shell) ions. Although the X-ray crystal structure and EXAFS analyses demonstrated the Cu−Cu distance to be 2.6 Å in 1YEW,[11a] the present DFT results are not in good agreement with the experimental observations. A computed Cu−Cu distance in the possible starting $Cu^{I}Cu^{I}$ state is 3.632 Å. A possible reason for this long Cu−Cu distance in the $Cu^{I}Cu^{I}$ state would be a Coulomb repulsion between the two Cu^{I} ions. However, experimental observations are not fully consistent about the Cu−Cu distance of the dicopper site. For example, it is 3.127 Å in 3CHX, 2.709 Å in 3RFR, and 2.666 Å in 3RGB.[11c,d] By inserting a dioxygen molecule, **PO** is formed in either a triplet or an open-shell singlet spin state corresponding to ferromagnetically and antiferromagnetically coupled Cu^{II} (d^9) ions, respectively. Calculated energies of **PO** in the triplet state and the singlet state are 3.3 and 2.9 kcal/mol, respectively, relative to the dissociation limit of **RED** and O_2. Thus, the oxygen insertion can easily occur in **RED**. The four Cu−O bond distances range from 1.96 to 2.09 in the Cu_2O_2 core. The Cu−Cu distance of 3.385 Å in **PO** is shorter than the Cu−Cu of 3.632 Å in **RED**. The short Cu−O_{Tyr} distance, 2.217 Å, indicates that the tyrosine residue is a part of the first coordination sphere of the copper atom in **PO**. In synthetic model studies the Cu−Cu distance of μ-η^2:η^2-peroxo$Cu^{II}Cu^{II}$ complexes is 3.5 Å in general and the Cu_2O_2 core is planar in structure.[33] In contrast, the short Cu−Cu distance in intermediate **PO** can lead to the formation of a bent-butterfly structure in the Cu_2O_2 core. We could not obtain a planar structure for the peroxo species in the DFT calculations at the B3LYP* level of theory; the bent-butterfly structure is energetically more favorable in this peroxo species. Karlin and co-workers[22a] demonstrated from X-ray absorption and Raman spectroscopy that a peroxide-bridged dicopper core $[Cu_2(\mu\text{-}\eta^2\text{:}\eta^2(O_2))]^{2+}$ shows a bent-butterfly structure. According to the orbital interaction analysis,[22d] the next highest occupied molecular orbital (HOMO) of the planar structure involves a nonbonding interaction between the two Cu $d_{x^2-y^2}$ orbitals and the out-of-plane peroxide (π^*_v) orbital; this orbital is significantly stabilized in energy in the butterfly structure because of the increased interaction between the two Cu $d_{x^2-y^2}$ orbitals and the peroxide π^*_v orbital. Thus, our DFT result about the butterfly structure is in good agreement with their spectroscopic and orbital interaction studies on the $[Cu_2(\mu\text{-}\eta^2\text{:}\eta^2(O_2))]^{2+}$ core. The calculated O−O bond distance of 1.424 Å is in reasonable agreement with the available experimental values for peroxo-metal complexes, and it is, of course, longer than the 1.207 Å of the O−O double bond in the dioxygen molecule. The cleavage of the O−O bond in **PO** leads to the formation of **BMO**. As a result, the O−O distance increases from 1.424 Å in **PO** to 2.317 Å and the Cu−Cu distance decreases to 2.752 Å in **BMO**. The Cu−O_{Tyr} distance increases from 2.217 Å in **PO** to 2.639 Å in **BMO**, indicating the lack of a strong coordination bond to the Tyr residue.

dx.doi.org/10.1021/ic400417d | *Inorg. Chem.* 2013, 52, 7907−7917

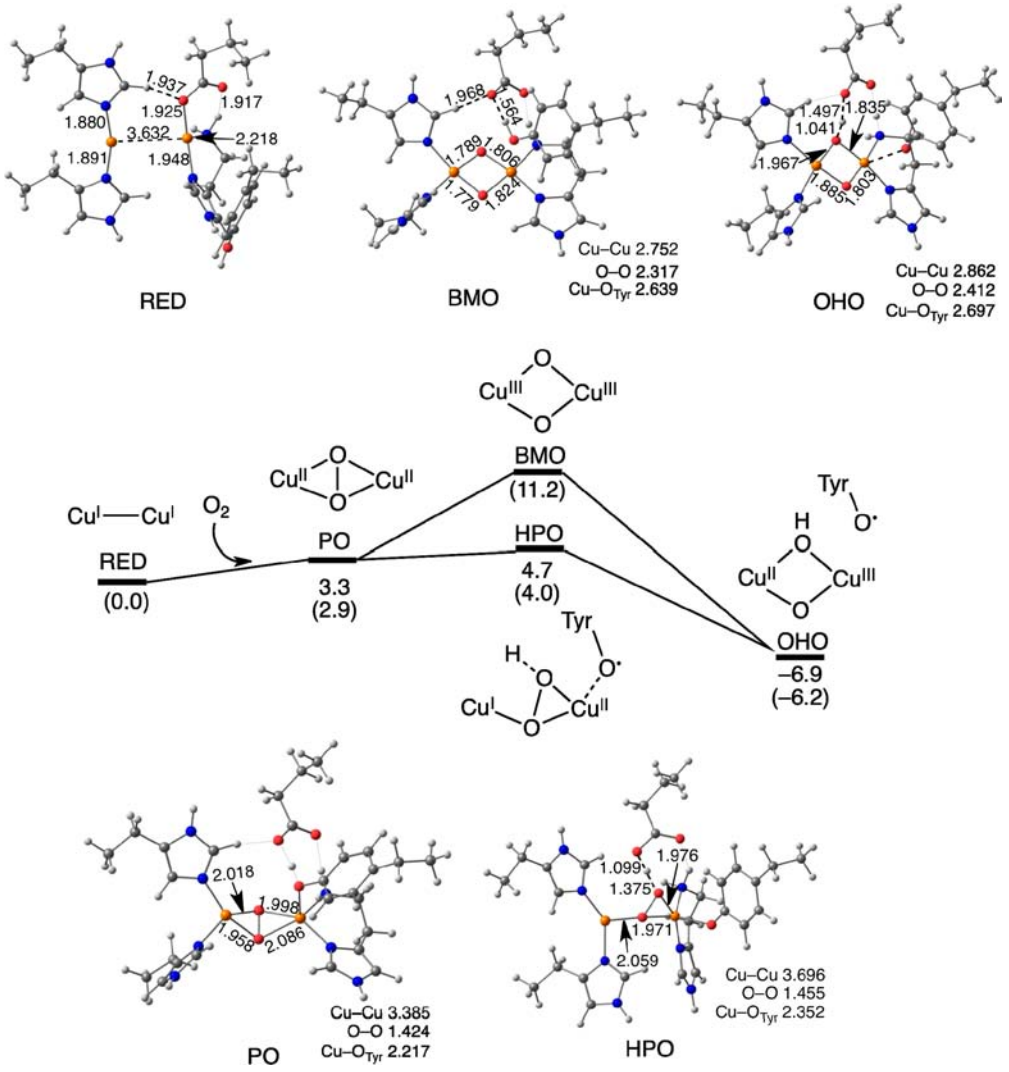

Figure 2. Optimized structures and computed energies of $Cu^{I}Cu^{I}$ (**RED**), μ-η^2:η^2-peroxo$Cu^{II}Cu^{II}$ (**PO**), μ-η^1:η^2-hydroperoxo$Cu^{I}Cu^{II}$ (**HPO**), bis(μ-oxo)$Cu^{III}Cu^{III}$ (**BMO**), and (μ-oxo)(μ-hydroxo)$Cu^{II}Cu^{III}$ (**OHO**) in the triplet state. The values are corrected by zero-point vibrational energies and Gibbs free energies. The values in parentheses are energies in the singlet state. Units are in kcal/mol and Å.

In the singlet state the energy difference between **BMO** and **PO**, the O−O bond dissociation step, is 8.3 kcal/mol. In our previous calculations on a different model of (Cu_2O_2)-$(acetate)_2(imid)_3$, the energy difference was 14.7 kcal/mol. Cramer et al.[34] reported the bis(μ-oxo)$Cu^{III}Cu^{III}$ species to be 8.3 kcal/mol at the BLYP/TZP level and 27.3 kcal/mol at the B3LYP/TZP level above the peroxo$Cu^{II}Cu^{II}$ species using a small model of $(Cu_2O_2)(imid)_6$ in the singlet state. Although the corresponding energy difference strongly depends on DFT functionals used and ligands in dicopper models, these DFT analyses clearly indicate that the bis(μ-oxo)$Cu^{III}Cu^{III}$ species tends to have higher free enthalpy than the corresponding μ-η^2:η^2-peroxo$Cu^{II}Cu^{II}$ species. According to the CASPT2 calculation of Flock and Pierloot,[35] the bis(μ-oxo)$Cu^{III}Cu^{III}$ species is 12.7 kcal/mol more stable than the μ-η^2:η^2-peroxo$Cu^{II}Cu^{II}$ species using a simple model of (Cu_2O_2)-$(NH_3)_6$ in contrast to the DFT results. Gherman and Cramer[34d] suggested that the latter calculations are not correct, because of an error in the second-order perturbation (PT2) correction.

Other DFT analyses as well as our B3LYP* results demonstrate that the bis(μ-oxo)$Cu^{III}Cu^{III}$ species tends to have higher free enthalpy than the corresponding μ-η^2:η^2-peroxo$Cu^{II}Cu^{II}$ species. Liakos and Neese[36] reported that only at a high level of theory involving complete basis set extrapolation, triple excitation contributions, relativistic effects, and solvent effects, the bis(μ-oxo)$Cu^{III}Cu^{III}$ structure is found to be slightly more stable than the peroxo structure. In summary, the reasonable estimation of the energy difference between the bis(μ-oxo)$Cu^{III}Cu^{III}$ species and the μ-η^2:η^2-peroxo$Cu^{II}Cu^{II}$ species has been a challenging target of theoretical chemistry for a long time. The energy difference is not readily assessed by DFT calculations. In a previous study,[32] we showed that the μ-η^2:η^2-peroxo$Cu^{II}Cu^{II}$ species is able to abstract an H atom from tyrosine to form a hydroperoxo$Cu^{I}Cu^{II}$ species with a very low activation barrier. On the basis of this result, we propose here that the possible H-atom transfer from Tyr374 to the μ-η^2:η^2-peroxo$Cu^{II}Cu^{II}$ species can lead to the formation of the (μ-oxo)(μ-hydroxo)-$Cu^{II}Cu^{III}$ intermediate, the reactivity of which is our main interest in this work.

The cleavage of the O_{Tyr}-H bond in **PO** leads to the formation of **HPO**, a μ-η^1:η^2-hydroperoxo $Cu^{I}Cu^{II}$ species with a phenoxyl radical and a protonated peroxo ligand. One of the

dx.doi.org/10.1021/ic400417d | Inorg. Chem. 2013, 52, 7907−7917

Scheme 2

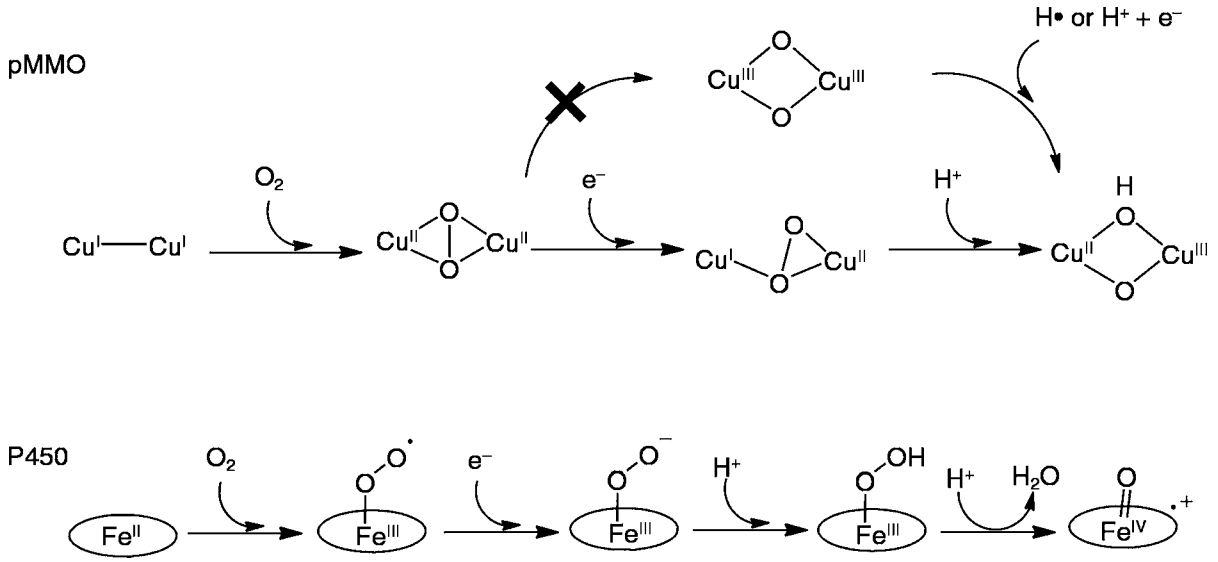

Table 1. Calculated Mulliken Spin Populations (Atomic Charges) in the Cu_2O_2 Core

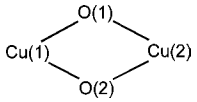

	spin state	$\langle S^2\rangle^c$	Cu(1)	Cu(2)	O(1)	O(2)
RED	singlet[a]	0.000	0.00 (0.51)	0.00 (0.48)		
PO	triplet	2.000	0.40 (0.32)	0.47 (0.39)	0.45 (−0.23)	0.42 (−0.25)
PO	singlet[b]	0.040	0.40 (0.32)	−0.47 (0.39)	0.06 (−0.24)	0.07 (−0.26)
BMO	singlet[a]	0.000	0.00 (0.28)	0.00 (0.39)	0.00 (−0.43)	0.00 (−0.51)
HPO	triplet	2.000	0.03 (0.14)	0.41 (0.30)	0.24 (−0.38)	0.23 (−0.36)
HPO	singlet[b]	0.196	0.03 (0.14)	0.40 (0.30)	0.23 (−0.38)	0.22 (−0.36)
OHO	triplet	2.003	0.53 (0.33)	−0.07 (0.34)	0.13(−0.17)[d]	0.32 (−0.54)
OHO	singlet[b]	0.446	0.53(0.33)	−0.07(0.34)	0.13(−0.17)[d]	0.32 (−0.54)

[a]Closed-shell singlet. [b]Open-shell singlet. [c]$\langle S^2\rangle$ after annihilation. [d]Hydroxo oxygen.

Cu−O bond distances increases from 2.018 Å to 3.109 Å, whereas the O−O bond distance and the three other Cu−O bond distances remain unchanged. The O_{Cu}-H and O_{Glu}-H bond distances are 1.375 and 1.099 Å, respectively. Although the H atom derived from the tyrosine residue is shared by the Cu_2O_2 and glutamate moieties, **HPO** can be viewed as a μ-η^1:η^2-peroxoCu^ICu^{II} form rather than a μ-η^1:η^2-hydroperoxoCu^ICu^{II} form because of the long OH distance (1.375 Å). The H radical species generated by the homolytic cleavage of the H−O_{Tyr} bond gives rise to a simultaneous electron and proton transfer. As a result, the Cu_2O_2 core and the Glu moiety work as an electron acceptor and a proton acceptor, respectively. The energy difference between **PO** and **HPO** is only 1.4 kcal/mol in the triplet state and 1.1 kcal/mol in the open-shell single state, while the calculated energy of **BMO** is 8.3 kcal/mol higher than **PO** in the singlet state. Thus, the formation of **HPO** species is energetically favored.

In addition to the homolytic O_{Tyr}-H bond dissociation, the O−O bond dissociation easily occurs in **HPO** concomitant with the formation of oxo and hydroxo bridges, resulting in the formation of the (μ-oxo)(μ-hydroxo)$Cu^{II}Cu^{III}$ species, **OHO**. After dioxygen insertion, the Cu−O_{Tyr} distance is decreased to 2.217 Å in **PO** and 2.352 Å in **HPO**, as shown in Figure 2. The tyrosine residue in the peroxo species can interact with the Cu_2O_2 core as an H-atom donor. This mechanism is possible in pMMO because Tyr374 is located in the second coordination sphere of the dicopper site. In fact, the Cu−O_{Tyr} distance in the X-ray structural analysis before dioxygen insertion (**RED** in our notation) is about 5 Å in 1YEW, 3RFR, and 3RGB and 8 Å in 3CHX.[11] From this computational result we suggest that this highly reactive dicopper species can be formed if the phenol moiety of the Tyr374 residue accesses the dicopper site in the coordination environment. The longest Cu−O distance in the diamond core is remarkably decreased to 1.967 Å in **OHO** from 3.109 Å in **HPO**, and the O−O and Cu−Cu distances are 2.412 and 2.862 Å, respectively. In **OHO**, the bridging hydroxo ligand forms two Cu−O bonds of 1.967 and 1.835 Å. The bridging oxo ion, which can abstract a hydrogen atom from methane, has two Cu−O bonds of 1.885 and 1.803 Å. The O_{Cu}-H and O_{Glu}-H distances change from 1.375 and 1.099 Å in **HPO** to 1.041 and 1.497 in **OHO**, respectively, which indicates the migration of the H atom to the oxygen atom of the Cu_2O_2 moiety. A calculated energy of **OHO** is −6.9 kcal/mol, which makes it the most stable copper species among the calculated species, **PO**, **BMO**, **HPO**, and **OHO**. The electron transfer to the Cu_2O_2 moiety in **PO** induces the O−O bond activation to form the stable μ-oxo complex via **HPO** because **BMO** lies 11.2 kcal/mol above **HPO**. Computed energies of **BMO** and **OHO** at the B3LYP* level suggest that electron transfer and protonation induce the O−O bond dissociation. Scheme 2

dx.doi.org/10.1021/ic400417d | Inorg. Chem. 2013, 52, 7907−7917

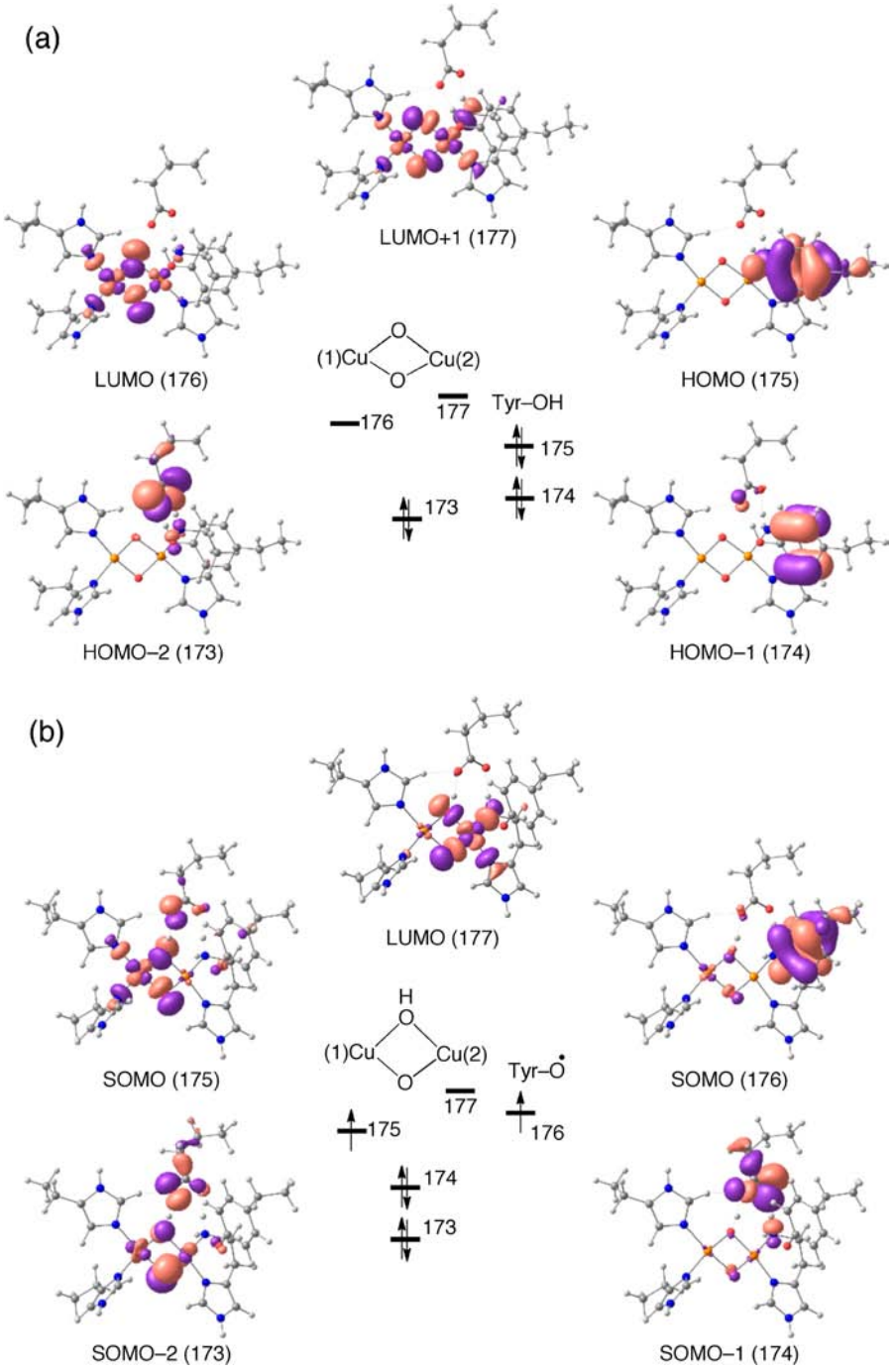

Figure 3. Molecular orbitals from α-173 to 177 in (a) **BMO** of the singlet state and (b) **OHO** of the triplet state.

indicates possible O−O bond activation pathways of pMMO and cytochrome P450.[37] These pathways involve a dissociative activation initiated by protonation, which is widely believed to occur in metalloenzymes in general. Considering the changes in the electronic structures of the Cu_2O_2 moiety of pMMO, a plausible pathway for the formation of **OHO** proceeds in the order of dioxygen insertion and one-electron transfer followed by protonation. Without electron transfer and protonation, the O−O bond dissociation would be an energetically unfavorable process.

To monitor the electronic structure of the dioxygen molecule along the reaction, we calculated the Mulliken populations (spin and charge) for all the steps, as summarized in Table 1. The spin density distribution clearly reflects the electronic features and bonding along the reaction pathway from **PO** to **OHO**. Calculated spin densities of **PO** at the Cu(1), Cu(2), O(1), and O(2) atoms are 0.40, 0.47, 0.45, and 0.42, respectively, in the triplet state, and 0.40, −0.47, 0.06, and 0.07, respectively, in the open-shell singlet state. The triplet and singlet states correspond to the ferromagnetically and antiferromagnetically coupled d^9 electronic configurations, respectively. The closed-shell singlet state is the ground state in **BMO** with no spin density in the Cu_2O_2 moiety. This Mulliken population analysis indicates that the formal charges (Mulliken atomic charges) of the Cu(1) and Cu(2) atoms are +2 (0.32) and +2 (0.39) in **PO** and +3 (0.28) and +3 (0.39) in

dx.doi.org/10.1021/ic400417d | *Inorg. Chem.* 2013, 52, 7907−7917

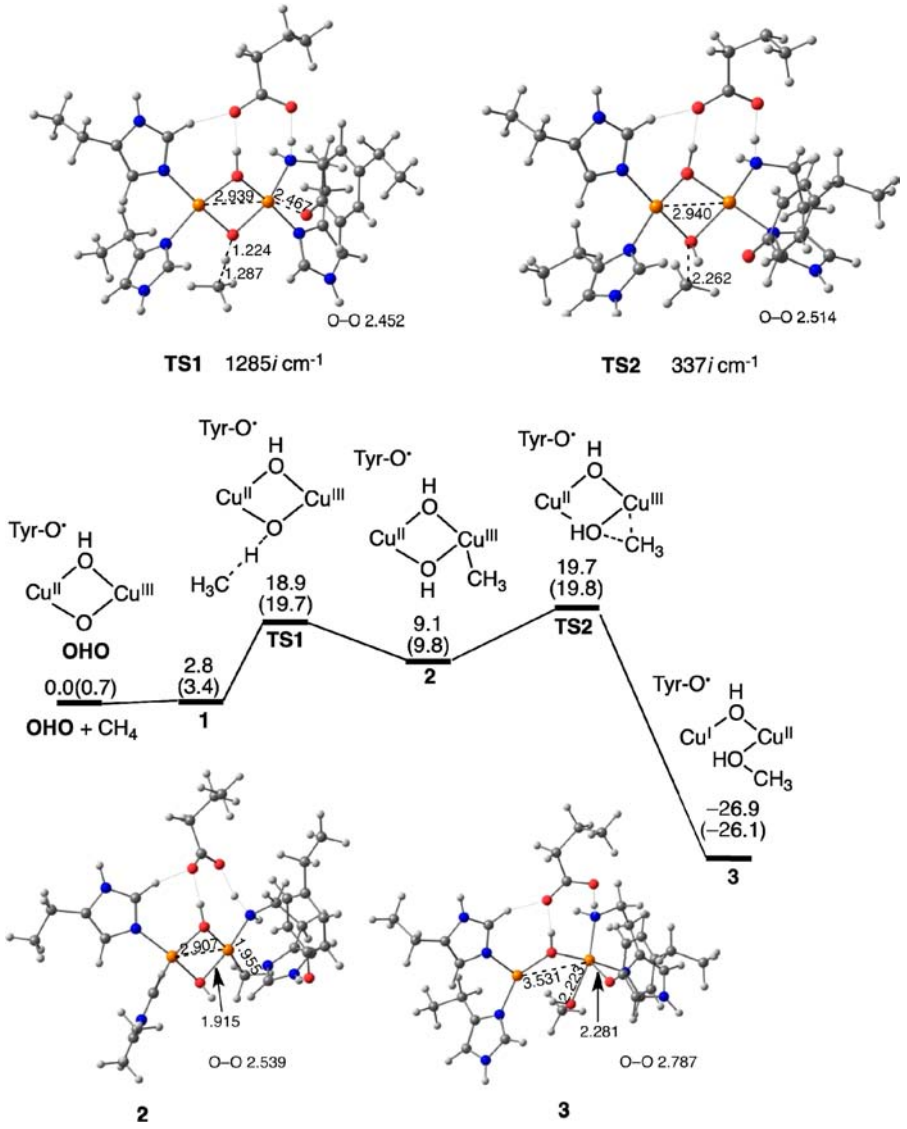

Figure 4. Energy diagram for methane hydroxylation with relative energies (triplet state) calculated from the dissociation limit of **OHO** + CH_4. The values are corrected by zero-point vibrational energies and Gibbs free energies. The values in parentheses are energies in the singlet state. Units are in kcal/mol and Å.

BMO, respectively. The Mulliken atomic charges are less effective in assigning the oxidation state of Cu in the Cu_2O_2 species compared to the Mulliken atomic spin densities in general. In the triplet state calculated spin densities of **HPO** at the Cu(1), Cu(2), O(1), and O(2) atoms are 0.03, 0.41, 0.24, and 0.23, respectively. The spin density of 0.24 at the O(1) atom, instead of 0.0, indicates that the bonding between the O(1) atom and the shared H atom is weak, which is consistent with the long H−O(1) distance of 1.375 Å. Considering that the total amount of spin densities in the Cu_2O_2 moiety is decreased to 0.91 in **HPO** from 1.74 in **PO**, the formal charges of the Cu(1) and Cu(2) atoms are +1 and +2 in **HPO**. In the open-shell singlet state, the Mulliken spin densities are identical to the corresponding values of the triplet state, with the exception of the phenoxyl radical. These results show that the electronic configurations of **HPO** in the triplet and singlet states correspond to the ferromagnetically and antiferromagnetically coupled pairs of the μ-η^1:η^2-peroxo Cu^ICu^{II} species and the phenoxyl radical, respectively. The O−O bond dissociation increases the formal charges of Cu(1) and Cu(2) atoms because of the oxidation process. Since calculated spin densities of the Cu(1) and Cu(2) atoms are 0.53 and −0.07, respectively, the formal charges of the Cu(1) and Cu(2) atoms can be assigned to be +2 and +3 in **OHO**. The H-atom migration to the O(1) atom decreases the spin density to form a closed-shell configuration. The (μ-oxo)(μ-hydroxo)$Cu^{II}Cu^{III}$ species is essentially viewed as a doublet species because the tyrosyl radical is only weakly coupled. Since the total spin density remains unchanged in **OHO**, the O(2) atom spin density increases to 0.32 in **OHO** from 0.23 in **HPO**. Intermediate **OHO** has a large spin density in the oxo-bridge compared to **HPO**. At the same time, the H-atom migration occurring in the **PO** species is responsible for the formation of **OHO**, which is 10.2 kcal/mol below the energy of **PO**. Therefore we expect that **OHO**, which involves a tyrosine residue at the second coordination sphere, is a good initiator for the active species for methane hydroxylation.

The different reactivity of **BMO** and **OHO** can be understood if we take a look at the molecular orbitals from 173 to 177 in (a) **BMO** of the singlet state and (b) **OHO** of the

dx.doi.org/10.1021/ic400417d | Inorg. Chem. 2013, 52, 7907−7917

Table 2. Relative Energies for Methane Oxidation by Dicopper Species at the B3LYP* Level

species	ΔG(Oxo)[a]	$\Delta G^{\ddagger}$(TS1)[b]	$\Delta G^{\ddagger}$(TS2)[c]	ΔG(3-1)[d]
bis(μ-oxo)$Cu^{III}Cu^{III}$	7.9	9.5	24.0	−54.0
bis(μ-oxo)$Cu^{II}Cu^{III}$	2.5	14.2	25.0	−45.3
(μ-oxo)(μ-hydroxo)$Cu^{II}Cu^{III}$	−10.2	16.1	10.6	−29.7

[a] ΔG(Oxo) = G(Peroxo) − G(Oxo). [b] The activation free energy ($\Delta G^{\ddagger}$) of **TS1**. [c] The activation free energy ($\Delta G^{\ddagger}$) of **TS2**. [d] Relative energies of **3** measured from reaction species.

triplet state, as shown in Figure 3. In **BMO** the LUMO(176) and LUMO+1(177) correspond to the mixture of the $d_{x^2-y^2}$ orbitals in the two Cu atoms and the p orbitals in the two bridging O atoms. The electronic structure of the Cu_2O_2 core explains that the bis(μ-oxo)$Cu^{III}Cu^{III}$ species has high affinity for an electron and low reactivity toward methane as it is generally known. Both unoccupied orbitals are Cu−O antibonding orbitals. When an electron in **BMO** transfers from the HOMO(175) to the LUMO(176) resulting in the SOMO(175) of **OHO**, this orbital would play a role in the C−H bond dissociation of methane. The resultant electronic structure is expected to have large spin density on the bridging oxygen atom so as to promote the C−H bond dissociation of methane. The HOMO-1(174) and HOMO(175) mainly come from the benzene ring of the tyrosine residue, and thus tyrosine residue is spatially a reactive species compared to the Cu_2O_2 core. The HOMO-2(173) is localized on the Glu moiety. In **OHO** the SOMO(175), SOMO(176), and LUMO(177) are localized in the $d_{x^2-y^2}$ orbital of the Cu(2) atom, the phenoxyl radical of tyrosine moiety, and $d_{x^2-y^2}$ orbital of the Cu(1) atom, respectively. This is fully consistent with the picture that the spin carriers are the Cu(1) atom and the phenoxyl radical. In contrast, the Cu(2) atom corresponding to the valence of +3 in the d^8 system has no spin density. The doubly occupied orbitals of the SOMO-1(174) and SOMO-2(173) are found in the glutamate ligand and the bridging oxygen atoms. The SOMO-2(173) involves the nonbonding p_z orbital of the oxygen bridge atoms. Since the σ^* orbital of the Cu−O bond in the SOMO(175) plays an important role in the H-atom abstraction from methane compared to the nonbonding p_z orbital, the equatorial position of the Cu_2O_2 core is more reactive compared to the axial position.

Hydroxylation of Methane by (μ-oxo)(μ-hydroxo)-$Cu^{II}Cu^{III}$. In previous studies,[5e,16] we concluded that the peroxo species and the bis(μ-oxo)$Cu^{III}Cu^{III}$ species have no direct ability to activate methane, while the bis(μ-oxo)$Cu^{II}Cu^{III}$ species can react with methane to activate the inert C−H bond methane. The reactions of the bis(μ-oxo)$Cu^{II}Cu^{III}$ species and the bis(μ-oxo)$Cu^{III}Cu^{III}$ species with methane were discussed in detail in previous papers.[5e,16] Here, let us take a look at the reactivity of the (μ-oxo)(μ-hydroxo)$Cu^{II}Cu^{III}$ species with respect to the hydroxylation of methane. Figure 4 shows computed energy diagrams along the reaction pathway starting from the dissociation limit (**OHO** and methane) to the methanol complex **3** that involves a tyrosine radical, a methanol ligand, and a (μ-hydroxo)$Cu^{I}Cu^{II}$ species in the triplet and singlet states. Since the reaction system retains a stable phenoxyl radical and an unpaired electron in the Cu_2O_2 moiety during the methane oxidation, we have considered the two spin states corresponding to the ferromagnetically and the antiferromagnetically coupled unpaired spins. The energy difference between the two spin states is small during the reaction pathway; therefore the energy profiles based on the two spin states are essentially identical. To avoid duplication of description, we refer to only the energies of the triplet state. The hydroxylation of methane by **OHO** starts with the formation of a methane complex (**1**). The first transition state (**TS1**) leads to the C−H bond dissociation of methane. A calculated activation energy of **TS1** is 16.1 kcal/mol relative to **1**. Compared with the bond dissociation energy of methane of about 104 kcal/mol, this activation is small enough for an enzymatic reaction that occurs under physiological conditions. The C−H bond dissociation of methane changes the O(−2) ligand and the neutral methane into the OH(−1) ligand and the CH_3(−1) ligand. Thus, the oxidation state of the dicopper site remains unchanged. The H-atom abstraction forms a methyl intermediate; no radical species is formed in this mechanism. This mechanistic proposal would be consistent with the experimental observation[38] that chiral ethane hydroxylation by pMMO from *Methylococcus capsulatus* (Bath) exhibits negligible racemization.

The energy diagram connects the methyl intermediate (**2**) and the methanol complex (**3**) via the second transition state (**TS2**) in the C−O bond formation step. A calculated activation energy for **TS2** is 10.6 kcal/mol relative to **2**. Since the calculated activation energy of **TS2** is lower than that of **TS1**, the rate-determining step is the C−H bond dissociation in the methane hydroxylation. These calculated activation barriers are consistent with experimental KIE (k_H/k_D) values of 5.2−5.5 at 30 °C in ethane hydroxylation by pMMO.[38]

Finally, we would like to look at the energy profiles for the methane hydroxylation by possible dicopper species. Table 2 lists computed formation energies of the active oxo species from the corresponding peroxo species and hydroperoxo species, activation free energies for the C−H cleavage (**TS1**) and rebound (**TS2**) steps, and total reaction energies of the methane hydroxylation. Calculated relative energies of the methanol complex **3** measured from the methane complex (ΔG(**3**-**1**)) are −54.0, −45.3, and −29.7 kcal/mol for the bis(μ-oxo)$Cu^{III}Cu^{III}$, bis(μ-oxo)$Cu^{II}Cu^{III}$, and (μ-oxo)(μ-hydroxo)-$Cu^{II}Cu^{III}$ species, respectively. Therefore the methane hydroxylation catalyzed by the three dicopper species is all exothermic. However, the μ-η^2:η^2-peroxo$Cu^{II}Cu^{II}$ species and the bis(μ-oxo)$Cu^{III}Cu^{III}$ species have no reactivity to the C−H activation of methane, as mentioned earlier. We previously suggested that two active species are able to carry out methane hydroxylation; one is the bis(μ-oxo)$Cu^{II}Cu^{III}$ species[5e,16] derived from the μ-η^1:η^2-peroxo$Cu^{I}Cu^{II}$ species and another is the single-bridged (μ-oxo)$Cu^{II}Cu^{III}$ species[16b] derived from the dissociation of one Cu−O bond in the bis(μ-oxo)$Cu^{III}Cu^{III}$ species. The Cu−O moiety is a highly reactive species and considered as a good oxygen donor.[39−42] However, since the dissociation of one Cu−O bond in the bis(μ-oxo)$Cu^{III}Cu^{III}$ species requires more than 21 kcal/mol relative to the μ-η^2:η^2-peroxo$Cu^{II}Cu^{II}$ species, the single-bridged (μ-oxo)$Cu^{II}Cu^{III}$ species would be thermally not accessible under physiological conditions. In contrast, the formations of the bis(μ-oxo)$Cu^{II}Cu^{III}$ species and the (μ-oxo)(μ-hydroxo)$Cu^{II}Cu^{III}$ species require lower ΔG(Oxo)

dx.doi.org/10.1021/ic400417d | Inorg. Chem. 2013, 52, 7907−7917

values of 2.5 and −10.2 kcal/mol, respectively. Calculated activation energies for the C−H bond activation, $\Delta G^{\ddagger}$(**TS1**), are 9.5 kcal/mol, 14.2 kcal/mol, and 16.1 kcal/mol for the (μ-oxo)$Cu^{III}Cu^{III}$, bis(μ-oxo)$Cu^{II}Cu^{III}$, and (μ-oxo)(μ-hydroxo)-$Cu^{II}Cu^{III}$ species, respectively. Thus, these dicopper centers can activate the strong C−H bond of methane. However, the single-bridged (μ-oxo)$Cu^{II}Cu^{III}$ species should not be formed under physiological conditions, as mentioned above. Calculated $\Delta G^{\ddagger}$(**TS2**) values, which correspond to the rebound step, for the bis(μ-oxo)$Cu^{II}Cu^{III}$ species and the (μ-oxo)(μ-hydroxo)-$Cu^{II}Cu^{III}$ species are 25.0 and 10.6 kcal/mol, respectively. The $\Delta G^{\ddagger}$(**TS2**) value of 10.6 kcal/mol for the (μ-oxo)(μ-hydroxo)-$Cu^{II}Cu^{III}$ species is lower than the $\Delta G^{\ddagger}$(**TS1**) value of 16.1 kcal/mol, which is fully consistent with the observed KIE values suggesting that the C−H cleavage of methane is the rate-determining step. As a result, only the calculated reaction profile with (μ-oxo)(μ-hydroxo)$Cu^{II}Cu^{III}$ species as an intermediate (Figure 4) is likely to be consistent with the experimental findings. In this mechanism, the tyrosine residue in the second coordination sphere of the dicopper site should play an essential role in the formation of the active species to react with methane in the pMMO enzyme.

CONCLUSIONS

We have investigated the reactivity of the (μ-oxo)(μ-hydroxo)-$Cu^{II}Cu^{III}$-type active species of pMMO by turning our attention to the role of the tyrosine residue in the second coordination sphere of the dicopper site in the oxygen activation process on the basis of the H-atom migration from tyrosine substrate proposed for the oxidation of tyrosine to dopaquinone.[32] In our previous studies,[5e,16] we reported that based on DFT calculations the bis(μ-oxo)$Cu^{II}Cu^{III}$ species can activate methane in contrast to the bis(μ-oxo)$Cu^{III}Cu^{III}$ species. We concluded that the acceptance of one electron by the Cu_2O_2 core is important to the methane activation by pMMO. The H-atom transfer discussed in the present work is equivalent of the transfer of electron and proton to the bis(μ-oxo)$Cu^{III}Cu^{III}$ species; the (μ-oxo)(μ-hydroxo)$Cu^{II}Cu^{III}$ species as well as the bis(μ-oxo)$Cu^{II}Cu^{III}$ species shows high reactivity to methane. We propose that the H-atom transfer is responsible for the O−O bond activation and the formation of the (μ-oxo)(μ-hydroxo)$Cu^{II}Cu^{III}$ species in pMMO. Since the energy of the (μ-oxo)(μ-hydroxo)$Cu^{II}Cu^{III}$ species is −10.2 kcal/mol relative to the corresponding hydroperoxo species, the occurrence of the oxo-hydroxo form is energetically favored. DFT calculations demonstrated that the conversion of methane to methanol takes place in a two-step manner. The first transition state that leads to the C−H bond dissociation of methane requires an activation energy of 16.1 kcal/mol relative to the reactant complex. This H-atom abstraction results in the formation of a methyl intermediate without a radical species. The second transition state leads to the C−O bond formation, which is the so-called oxygen-rebound step in bioinorganic chemistry. The energy of the second transition state is 10.6 kcal/mol measured from the methyl intermediate. Since the second activation barrier is lower than the first one, the rate-determining step is likely to be the C−H bond dissociation step in the methane hydroxylation. Finally we propose that the enzymatic function will be lost if the tyrosine residue is mutated. More detailed studies on how the protein environment may shift the stability of the various Cu−Cu species and how it may influence the availability of different reaction pathways are in progress.

ASSOCIATED CONTENT

Supporting Information

Complete ref 30 and atomic Cartesian coordinates for all the structures optimized in the present study. This material is available free of charge via the Internet at http://pubs.acs.org.

AUTHOR INFORMATION

Corresponding Author

*E-mail: kazunari@ms.ifoc.kyushu-u.ac.jp.

Notes

The authors declare no competing financial interest.

ACKNOWLEDGMENTS

We thank Grants-in-Aid for Scientific Research (Nos. 21750063, 2245028, and 24109014) from the Japan Society for the Promotion of Science and the Ministry of Education, Culture, Sports, Science and Technology (MEXT) of Japan and the MEXT Projects of Integrated Research on Chemical Synthesis and Elements Strategy Initiative for their support of this work.

REFERENCES

(1) Colby, J.; Dalton, H.; Wittenbury, R. *Annu. Rev. Microbiol.* **1979**, *33*, 481.

(2) Anthony. C. *The Biochemistry of Metylotrophs*; Academic Press: London, U.K., 1982; pp 296−379.

(3) (a) Rostrup-Nielsen, J. R. *J. Catal.* **1973**, *31*, 173. (b) Xu, J.; Froment, G. F. *AIChE J.* **1989**, *35*, 88.

(4) (a) Feig, A. L.; Lippard, S. J. *Chem. Rev.* **1994**, *94*, 759. (b) Lipscomb, J. D. *Annu. Rev. Microbiol.* **1994**, *48*, 371. (c) Wallar, B. J.; Lipscomb, J. D. *Chem. Rev.* **1996**, *96*, 2625. (d) Que, L., Jr.; Dong, Y. *Acc. Chem. Res.* **1996**, *29*, 190. (e) Merkx, M.; Kopp, D. A.; Sazinsky, M. H.; Blazyk, J. L.; Muller, J.; Lippard, S. J. *Angew. Chem., Int. Ed.* **2001**, *40*, 2782.

(5) (a) Yoshizawa, K.; Yamabe, T.; Hoffmann, R. *New J. Chem.* **1997**, *21*, 151. (b) Yoshizawa, K.; Ohta, T.; Yamabe, T.; Hoffmann, R. *J. Am. Chem. Soc.* **1997**, *119*, 12311. (c) Yoshizawa, K. *J. Biol. Inorg. Chem.* **1998**, *3*, 318. (d) Yoshizawa, K.; Ohta, T.; Yamabe, T. *Bull. Chem. Soc. Jpn.* **1998**, *71*, 1899. (e) Yoshizawa, K.; Suzuki, A.; Shiota, Y.; Yamabe, T. *Bull. Chem. Soc. Jpn.* **2000**, *73*, 815. (f) Yoshizawa, K. *J. Inorg. Biochem.* **2000**, *78*, 23. (g) Yoshizawa, K.; Yumura, T. *Chem.—Eur. J.* **2003**, *9*, 2347. (h) Yoshizawa, K. *Acc. Chem. Res.* **2006**, *39*, 375.

(6) (a) Siegbahn, P. E. M.; Crabtree, R. H. *J. Am. Chem. Soc.* **1997**, *119*, 3103. (b) Siegbahn, P. E. M.; Crabtree, R. H.; Nordlund, P. *J. Biol. Inorg. Chem.* **1998**, *3*, 314. (c) Siegbahn, P. E. M. *Inorg. Chem.* **1999**, *38*, 2880. (d) Siegbahn, P. E. M.; Blomberg, M. R. A. *Chem. Rev.* **2000**, *100*, 421. (e) Siegbahn, P. E. M. *J. Biol. Inorg. Chem.* **2001**, *6*, 27.

(7) (a) Basch, H.; Mogi, K.; Musaev, D. G.; Morokuma, K. *J. Am. Chem. Soc.* **1999**, *121*, 7249. (b) Basch, H.; Musaev, D. G.; Mogi, K.; Morokuma, K. *J. Phys. Chem. A* **2001**, *105*, 3615. (c) Basch, H.; Musaev, D. G.; Morokuma, K. *J. Phys. Chem. B* **2001**, *105*, 8452. (d) Torrent, M.; Musaev, D. G.; Basch, H.; Morokuma, K. *J. Comput. Chem.* **2002**, *23*, 59.

(8) (a) Dunietz, B. D.; Beachy, M. D.; Cao, Y.; Whittington, D. A.; Lippard, S. J.; Friesner, R. A. *J. Am. Chem. Soc.* **2000**, *122*, 2828. (b) Gherman, B. F.; Dunietz, B. D.; Whittington, D. A.; Lippard, S. J.; Friesner, R. A. *J. Am. Chem. Soc.* **2001**, *123*, 3836. (c) Guallar, V.; Gherman, B. F.; Miller, W. H.; Lippard, S. J.; Friesner, R. A. *J. Am. Chem. Soc.* **2002**, *124*, 3377. (d) Baik, M.-H.; Newcomb, M.; Friesner, R. A.; Lippard, S. J. *Chem. Rev.* **2003**, *103*, 2385.

(9) Chan, S. I.; Chen, K. H.-C.; Yu, S. S.-F.; Chen, C.-Li; Kuo, S. S.-J. *Biochemistry* **2004**, *43*, 4421.

(10) Lieberman, R. L.; Shrestha, D. B.; Doan, P. E.; Hoffman, B. M.; Stemmler, T. L.; Rosenzweig, A. C. *Proc. Natl. Acad. Sci. U.S.A.* **2003**, *100*, 3820.

(11) (a) Lieberman, R. L.; Rosenzweig, A. C. *Nature* **2005**, *434*, 177. (b) Lieberman, R. L.; Rosenzweig, A. C. *Acc. Chem. Res.* **2007**, *40*, 573. (c) Hakemian, A. S.; Kondapalli, K. C.; Telser, J.; Hoffman, B. M.; Stemmler, T. L.; Rosenzweig, A. C. *Biochemistry* **2008**, *47*, 6793. (d) Smith, S. M.; Rawat, S.; Telser, J.; Hoffman, B. M.; Stemmler, T. L.; Rosenzweig, A. C. *Biochemistry* **2011**, *50*, 10231.

(12) Lieberman, R. L.; Kondapalli, K. C.; Shrestha, D. B.; Hakemian, A. S.; Smith, S. M.; Telser, J.; Kuzelka, J.; Gupta, R.; Borovik, A. S.; Lippard, S. J.; Hoffman, B. M.; Rosenzweig, A. C.; Stemmler, T. L. *Inorg. Chem.* **2006**, *45*, 8372.

(13) (a) Choi, D.-W.; Kunz, R. C.; Boyd, E. S.; Semrau, J. D.; Antholine, W. E.; Han, J. I.; Zahn, J. A.; Boyd, J. M.; de la Mora, A. M.; DiSpirito, A. A. *J. Bacteriol.* **2003**, *185*, 5755. (b) Choi, D.-W.; Antholine, W. E.; Do, Y. S.; Semrau, J. D.; Kisting, C. J.; Kunz, R. C.; Campbell, D.; Rao, V.; Hartsel, S. C.; DiSpirito, A. A. *Microbiology.* **2005**, *151*, 3417. (c) Martinho, M.; Choi, D.-W.; DiSpirito, A. A.; Antholine, W. E.; Semrau, J. D.; Münck, E. *J. Am. Chem. Soc.* **2007**, *129*, 15783.

(14) (a) Chen, K. H.-C.; Chen, C.-L.; Tseng, C.-F.; Yu, S. S.-F.; Ke, S. C.; Lee, J.-F.; Nguyen, H.-H. T.; Elliott, S. J.; Alben, J. O.; Chan, S. I. *J. Chin. Chem. Soc.* **2004**, *51*, 1081. (b) Hung, S. C.; Chen, C.-L.; Chen, K. H.-C.; Yu, S. S.-F.; Chan, S. I. *J. Chin. Chem. Soc.* **2004**, *51*, 1229. (c) Chan, S. I.; Wang, V. C.-C.; Lai, J. C.-H.; Yu, S. S.-F.; Chen, P. P.-Y.; Chen, K. H.-C.; Chen, C.-L.; Chan, M. K. *Angew. Chem., Int. Ed.* **2007**, *46*, 1992. (d) Chan, S. I.; Yu, S. S.-F. *Acc. Chem. Res.* **2008**, *41*, 969. (e) Chan, S. I.; Lu, Y.-J.; Nagababu, P.; Maji, S.; Huang, M.-C.; Lee, M. M.; Hsu, I.-J.; Minh, P. D.; Lai, J. C.-H.; Ng, K. Y.; Ramalingam, S.; Yu, S. S.-F.; Chan, M. K. *Angew. Chem., Int. Ed.* **2013**, *52*, 3731.

(15) Balasubramanian, R.; Smith, S. M.; Rawat, S.; Yatsunyk, L. A.; Stemmler, T. L.; Rosenzweig, A. C. *Nature* **2010**, *465*, 115.

(16) (a) Yoshizawa, K.; Shiota, Y. *J. Am. Chem. Soc.* **2006**, *128*, 9873. (b) Shiota, Y.; Yoshizawa, K. *Inorg. Chem.* **2009**, *48*, 838.

(17) Chen, P. P.-Y.; Chan, S. I. *J. Inorg. Biochem.* **2006**, *100*, 801.

(18) (a) Yoshizawa, K.; Shiota, Y.; Yamabe, T. *Chem.—Eur. J.* **1997**, *3*, 1160. (b) Yoshizawa, K.; Shiota, Y.; Yamabe, T. *J. Am. Chem. Soc.* **1998**, *120*, 564. (c) Yoshizawa, K.; Shiota, Y.; Yamabe, T. *Organometallics* **1998**, *17*, 2825. (d) Shiota, Y.; Yoshizawa, K. *J. Am. Chem. Soc.* **2000**, *122*, 12317.

(19) (a) Schröder, D.; Schwarz, H. *Angew. Chem., Int. Ed. Engl.* **1995**, *34*, 1973. (b) Dietl, N.; van der Linde, C.; Maria Schlangen, M.; Beyer, M. K.; Schwarz, H. *Angew. Chem., Int. Ed.* **2011**, *50*, 4966.

(20) (a) Himes, R. A.; Karlin, K. D. *Curr. Opin. Chem. Biol.* **2009**, *13*, 119. (b) Himes, R. A.; Barnese, K.; Karlin, K. D. *Angew. Chem., Int. Ed.* **2010**, *49*, 6714.

(21) Woertink, J. S.; Smeets, P. J.; Groothaert, M. H.; Vance, M. A.; Sels, B. F.; Schoonheydt, R. A.; Solomon, E. I. *Proc. Natl. Acad. Sci. U.S.A.* **2009**, *106*, 18908.

(22) (a) Blackburn, N. J.; Strange, R. W.; Farooq, A.; Haka, M. S.; Karlin, K. D. *J. Am. Chem. Soc.* **1988**, *110*, 4263. (b) Pidcock, E.; Obias, H. V.; Zhang, X.; Karlin, K. D.; Solomon, E. I. *J. Am. Chem. Soc.* **1998**, *120*, 7841. (c) Obias, H. V.; Lin, Y.; Murthy, N. N.; Pidcock, E.; Solomon, E. I.; Ralle, M.; Blackburn, N. J.; Neuhold, Y.-M.; Zuberbühler, A. D.; Karlin, K. D. *J. Am. Chem. Soc.* **1998**, *120*, 12960. (d) Pidcock, E.; Obias, H. V.; Abe, M.; Liang, H.-C.; Karlin, K. D.; Solomon, E. I. *J. Am. Chem. Soc.* **1999**, *121*, 1299. (e) Kopf, M. A.; Karlin, K. D. Models of Copper Enzymes and Heme-Copper Oxidases. In *Biomimetic Oxidations Catalyzed by Transition Metal Complexes*; Muenier, B., Ed; Imperial College Press: London, U.K., 2000; pp 309–362. (f) Quant Hatcher, L.; Karlin, K. D. *J. Biol. Inorg. Chem.* **2004**, *9*, 669. (g) Lee, Y.; Karlin, K. D. In *Concepts and Models in Bioinorganic Chemistry*; Metzler-Nolte, N., Kraatz, H.-B., Eds.; Wiley-VCH: New York, 2006; pp 363–395. (h) Hatcher, L. Q.; Karlin, K. D. *Adv. Inorg. Chem.* **2006**, *58*, 131.

(23) (a) Halfen, J. A.; Mahapatra, S.; Wilkinson, E. C.; Kaderli, S.; Young, V. G., Jr.; Que, L., Jr.; Zuberbüler, A. D.; Tolman, W. B. *Science* **1996**, *271*, 1397. (b) Mahapatra, S.; Halfen, J. A.; Wilkinson, E. C.; Pan, G.; Wang, X.; Young, V. G., Jr.; Cramer, C. J.; Que, L., Jr.; Tolman, W. B. *J. Am. Chem. Soc.* **1996**, *118*, 11555. (c) Mahapatra, S.; Young, V. G., Jr.; Kaderli, S.; Zuberbüler, A. D.; Tolman, W. B. *Angew. Chem., Int. Ed. Engl.* **1997**, *36*, 130. (d) Que, L.; Tolman, W. B. *Angew. Chem., Int. Ed.* **2002**, *41*, 1114. (e) Aboelella, N. W.; Lewis, E. A.; Reynolds, A. M.; Brennessel, W. W.; Cramer, C. J.; Tolman, W. B. *J. Am. Chem. Soc.* **2002**, *124*, 10660. (f) Aboelella, N. W.; Kryatov, S. V.; Gherman, B. F.; Brennessel, W. W.; Young, V. G.; Sarangi, R.; Rybak-Akimova, E. V.; Hodgson, K. O.; Hedman, B.; Solomon, E. I.; Cramer, C. J.; Tolman, W. B. *J. Am. Chem. Soc.* **2004**, *126*, 16896. (g) Sarangi, R.; Aboelella, N.; Fujisawa, K.; Tolman, W. B.; Hedman, B.; Hodgson, K. O.; Solomon, E. *J. Am. Chem. Soc.* **2006**, *128*, 8286. (h) Brown, E. C.; Bar-Nahum, I.; York, J. T.; Aboelella, N. W.; Tolman, W. B. *Inorg. Chem.* **2007**, *46*, 486. (i) Hong, S.; Huber, S. M.; Gagliardi, L.; Cramer, C. C.; Tolman, W. B. *J. Am. Chem. Soc.* **2007**, *129*, 14190.

(24) Yumura, T.; Takeuchi, M.; Kobayashi, H.; Kuroda, Y. *Inorg. Chem.* **2009**, *48*, 508.

(25) (a) Itoh, S.; Nakao, H.; Berreau, L. M.; Kondo, T.; Komatsu, M.; Fukuzumi, S. *J. Am. Chem. Soc.* **1998**, *120*, 2890. (b) Taki, M.; Itoh, S.; Fukuzumi, S. *J. Am. Chem. Soc.* **2001**, *123*, 6203. (c) Itoh, S.; Kumei, H.; Taki, M.; Nagatomo, S.; Kitagawa, T.; Fukuzumi, S. *J. Am. Chem. Soc.* **2001**, *123*, 6708. (d) Itoh, S.; Fukuzumi, S. *Bull. Chem. Soc. Jpn.* **2002**, *75*, 2081. (e) Osako, T.; Ohkubo, K.; Taki, M.; Tachi, Y.; Fukuzumi, S.; Itoh, S. *J. Am. Chem. Soc.* **2003**, *125*, 11027. (f) Itoh, S. Dicopper enzymes. In *Comprehensive Coordination Chemistry II*; Que, L., Jr., Tolman, W. B., Eds.; Elsevier: Amsterdam, The Netherlands, 2004; Vol. *8*, pp 369–393. (g) Itoh, S.; Tachi, Y. *Dalton Trans.* **2006**, 4531.

(26) (a) Becke, A. D. *Phys. Rev. A* **1988**, *38*, 3098. (b) Lee, C.; Yang, W.; Parr, R. G. *Phys. Rev. B* **1988**, *37*, 785. (c) Becke, A. D. *J. Chem. Phys.* **1993**, *98*, 5648.

(27) (a) Reiher, M.; Salomon, O.; Hess, B. A. *Theor. Chem. Acc.* **2001**, *107*, 48. (b) Salomon, O.; Reiher, M.; Hess, B. A. *J. Chem. Phys.* **2002**, *117*, 4729.

(28) (a) Wachters, A. J. H. *J. Chem. Phys.* **1970**, *52*, 1033. (b) Hay, P. J. *J. Chem. Phys.* **1977**, *66*, 4377. (c) Raghavachari, K.; Trucks, G. W. *J. Chem. Phys.* **1989**, *91*, 1062.

(29) Dunning, T. H.; Hay, P. J. In *Modern Theoretical Chemistry*; Schaefer, H. F., III, Ed.; Plenum: New York, 1976; Vol. *3*, pp 1–27.

(30) Frisch, M. J. et al. *Gaussian 09*, Revision A.01; Gaussian, Inc.: Wallingford, CT, 2010.

(31) T. Inoue, T.; Shiota, Y.; Yoshizawa, K. *J. Am. Chem. Soc.* **2008**, *130*, 16890.

(32) (a) Quinlan, R. J.; Sweeney, M. D.; Leggio, L. L.; Otten, H.; Poulsen, J.-C. N.; Johansen, K. S.; Krogh, K. B. R. M.; Jørgensen, C. I.; Tovborg, M.; Anthonsen, A.; Tryfona, T.; Walter, C. P.; Xu, F.; Davies, G.; Walton, P. H. *Proc. Natl. Acad. Sci.* **2011**, *108*, 15079. (b) Aachmann, F. L.; Sørlie, M.; Skjåk-Bræk, G.; Eijsink, V. G. H.; Vaaje-Kolstad, G. *Proc. Natl. Acad. Sci.* **2012**, *109*, 18779.

(33) Mirica, L. M.; Ottenwaelder, X.; Stack, T. D. P. *Chem. Rev.* **2004**, *104*, 1013.

(34) (a) Cramer, C. J.; Woloch, M.; Piecuch, P.; Puzzarini, C.; Gagliardi, L. *J. Phys. Chem. A* **2006**, *110*, 1991. (b) Cramer, C. J.; Kinal, A.; Woloch, M.; Piecuch, P.; Gagliardi, L. *J. Phys. Chem. A* **2006**, *110*, 11557. (c) Lewin, J. L.; Heppner, D. E.; Cramer, C. J. *J. Biol. Inorg. Chem.* **2007**, *12*, 1221. (d) Gherman, B. F.; Cramer, C. J. *Coord. Chem. Rev.* **2009**, *253*, 723.

(35) Flock, M.; Pierloot, K. *J. Phys. Chem. A* **1999**, *103*, 95.

(36) Liakos, D. G.; Neese, F. *J. Chem. Theory Comput.* **2011**, *7*, 1511.

(37) Ortiz de Montellano, P. R. *Cytochrome P450: Structure, Mechanism, and Biochemistry*, 3rd ed.; Kluwer/Plenum: New York, 2005.

(38) Wilkinson, B.; Zhu, M.; Priestley, N. D.; Nguyen, H.-H. T.; Morimoto, H.; Williams, P. G.; Chan, S. I.; Floss, H. G. *J. Am. Chem. Soc.* **1996**, *118*, 921.

(39) Yoshizawa, K.; Kihara, N.; Kamachi, T.; Shiota, Y. *Inorg. Chem.* **2006**, *45*, 3034.

(40) Schröder, D.; Holthausen, M. C.; Schwarz, H. *J. Phys. Chem. B* **2004**, *108*, 14407.

(41) Solomon, E. I.; Decker, A. *Curr. Opin. Chem. Biol.* **2005**, *9*, 152.

(42) Comba, P.; Knoppe, S.; Martin, B.; Rajaraman, G.; Rolli, C.; Shapiro, B.; Stork, T. *Chem.—Eur. J.* **2008**, *14*, 344.